Published in final edited form as:
Bioorg Med Chem Lett. 2012 February 15; 22(4): 1541–1545. doi:10.1016/j.bmcl.2012.01.003.

Substitution of Gly with Ala enhanced the melanoma uptake of technetium-99m-labeled Arg-Ala-Asp-conjugated alpha-melanocyte stimulating hormone peptide

Jianquan Yang[a] and **Yubin Miao**[a,b,c,*]

[a]College of Pharmacy, Dermatology, University of New Mexico, Albuquerque, New Mexico 87131, USA

[b]Cancer Research and Treatment Center, Dermatology, University of New Mexico, Albuquerque, New Mexico 87131, USA

[c]Department of Dermatology, University of New Mexico, Albuquerque, New Mexico 87131, USA

Abstract

The purpose of this study was to determine the melanoma targeting property of ^{99m}Tc-RAD-Lys-(Arg^{11})CCMSH in B16/F1 melanoma-bearing C57 mice and compare with ^{99m}Tc-RGD-Lys-(Arg^{11})CCMSH we previously reported. ^{99m}Tc-RAD-Lys-(Arg^{11})CCMSH exhibited rapid and high tumor uptake (19.91 ± 4.02% ID/g at 2 h post-injection) in B16/F1 melanoma-bearing C57 mice. The tumor uptake of ^{99m}Tc-RAD-Lys-(Arg^{11})CCMSH was 1.51, 1.34 and 1.43 times the tumor uptake of ^{99m}Tc-RGD-Lys-(Arg^{11})CCMSH at 0.5, 2 and 4 h post-injection, respectively. Flank B16/F1 melanoma lesions were clearly imaged at 2 h post-injection using ^{99m}Tc-RAD-Lys-(Arg^{11})CCMSH as an imaging probe. The substitution of Gly with Ala significantly enhanced the melanoma uptake of ^{99m}Tc-RAD-Lys-(Arg^{11})CCMSH compared to ^{99m}Tc-RGD-Lys-(Arg^{11})CCMSH in B16/F1 melanoma-bearing C57 mice, providing a new insight into the design of α-MSH peptides for melanoma targeting.

Keywords

Arg-Ala-Asp-conjugated; alpha-melanocyte stimulating hormone peptide; melanocortin-1 receptor; receptor-targeting; melanoma imaging

Melanoma is the most deadly skin cancer with an increasing incidence. [1] Over the past decade, it has been of interest to develop receptor-targeting radiolabeled peptides for melanoma imaging since early diagnosis and prompt surgical removal is a patient's best opportunity for a cure. Due to the over-expression on melanoma, both melanocotin-1 (MC1) and $\alpha_v\beta_3$ integrin receptors have been used as targets for radiolabeled alpha-melanocyte stimulating hormone (α-MSH)[2-14] and Arg-Gly-Asp (RGD) peptides,[15-22] respectively. Recently, we have reported a novel RGD-conjugated α-MSH hybrid peptide targeting both MC1 and $\alpha_v\beta_3$ integrin receptors for M21 human melanoma imaging.[23] The cyclic RGD

[*]**Corresponding Author**: Yubin Miao, 2502 Marble NE, MSC09 5360, College of Pharmacy, University of New Mexico, Albuquerque, NM 87131. Phone: (505) 925-4437; Fax: (505) 272-6749; ymiao@salud.unm.edu.

{Arg-Gly-Asp-$_D$Tyr-Asp} motif was conjugated to [Cys^{3,4,10}, $_D$-Phe^7, Arg^{11}]α-MSH$_{3-13}$} peptide via a lysine linker to yield RGD-Lys-(Arg^{11})CCMSH hybrid peptide. Meanwhile, we designed two control peptides namely RAD-Lys-(Arg^{11})CCMSH and RGD-Lys-(Arg^{11})CCMSH$_{scramble}$ for comparison.[23] It is known that the switch from the RGD to RAD sacrifices the binding affinity of the RGD to the $\alpha_v\beta_3$ integrin receptor, whereas the motif of His-$_D$Phe-Arg-Trp is critical for strong MC1 receptor binding. The in vitro results revealed that the switch from RGD to RAD in the hybrid peptide decreased the $\alpha_v\beta_3$ integrin receptor binding affinity by 248-fold, whereas the scramble of CCMSH moiety in the hybrid peptide sacrificed the MC1 receptor binding affinity by 100-fold.[23] The biodistribution results demonstrated that targeting both MC1 and $\alpha_v\beta_3$ integrin receptors significantly enhanced the melanoma uptake of ^{99m}Tc-RGD-Lys-(Arg^{11})CCMSH in M21 human melanoma xenografts in our previous report.[23]

While the switch from RGD to RAD in the hybrid peptide decreased the $\alpha_v\beta_3$ integrin receptor binding affinity by 248-fold, surprisingly, we found that the switch from RGD to RAD in the hybrid peptide dramatically increased the MC1 receptor binding affinity of RAD-Lys-(Arg^{11})CCMSH compared to RGD-Lys-(Arg^{11})CCMSH (0.3 vs. 2.0 nM) in M21 melanoma cells in our previous report.[23] Therefore, we were interested in investigating whether such change in MC1 receptor binding affinity could lead to enhanced melanoma uptake of ^{99m}Tc-RAD-Lys-(Arg^{11})CCMSH compared to ^{99m}Tc-RGD-Lys-(Arg^{11})CCMSH. ^{99m}Tc-RGD-Lys-(Arg^{11})CCMSH targeted both MC1 and $\alpha_v\beta_3$ integrin receptors, whereas ^{99m}Tc-RAD-Lys-(Arg^{11})CCMSH only targeted the MC1 receptors. We chose B16/F1 melanoma cells for this study because only MC1 receptors (rather than $\alpha_v\beta_3$ integrin receptors) are over-expressed on B16/F1 cells.[24] Thus, selection of B16/F1 melanoma cells could minimize the contribution of $\alpha_v\beta_3$ integrin receptors to the melanoma uptake of dual receptor-targeting ^{99m}Tc-RGD-Lys-(Arg^{11})CCMSH.

In this study, RAD-Lys-(Arg^{11})CCMSH was synthesized, purified by RP-HPLC and characterized by electrospray ionization mass spectrometry according to our published procedure.[23] Schematic structure of RAD-Lys-(Arg^{11})CCMSH is presented in Figure 1. The structure of RGD-Lys-(Arg^{11})CCMSH was cited from our previous report[23] for comparison. The structural difference between RAD-Lys-(Arg^{11})CCMSH and RGD-Lys-(Arg^{11})CCMSH was one more methyl group in Ala compared to Gly (Fig. 1). The competitive binding curve of RAD- Lys-(Arg^{11})CCMSH in B16/F1 melanoma cells is presented in Figure 2. The MC1 receptor binding affinity of RAD-Lys-(Arg^{11})CCMSH was 0.26 nM in B16/F1 cells. Despite such slightly difference in structure, RAD-Lys-(Arg^{11})CCMSH displayed much stronger MC1 receptor binding affinity than RGD-Lys-(Arg^{11})CCMSH in B16/F1 melanoma cells (0.26 vs. 2.1 nM[24]). It suggested that the methyl group in Ala might somehow affect the MC1 receptor binding motif of His-$_D$Phe-Arg-Trp.

Cellular internalization and efflux of ^{99m}Tc-RAD-Lys-(Arg^{11})CCMSH in B16/F1 melanoma cells are presented in Figure 3. ^{99m}Tc-RAD-Lys-(Arg^{11})CCMSH exhibited rapid cellular internalization and extended cellular retention. There was 59.20 ± 5.10% of the ^{99m}Tc-RAD-Lys-(Arg^{11})CCMSH activity internalized at 20 min post incubation. There was 78.24 ± 1.13% of the ^{99m}Tc-RAD-Lys-(Arg^{11})CCMSH activity internalized after 2 h incubation. The efflux results demonstrated that 79.44 ± 3.61% of the ^{99m}Tc-RGD-Lys-(Arg^{11})CCMSH activity remained inside the cells 2 h after incubating cells in culture medium. Although ^{99m}Tc-RAD-Lys-(Arg^{11})CCMSH displayed similar rapid internalization and extended retention pattern as ^{99m}Tc- RGD-Lys-(Arg^{11})CCMSH,[24] more ^{99m}Tc-RAD-Lys-(Arg^{11})CCMSH activity was internalized and remained in B16/F1 melanoma cells in this study.

The melanoma targeting and pharmacokinetic properties of ^{99m}Tc-RAD-Lys-(Arg^{11})CCMSH were determined in B16/F1 melanoma-bearing C57 mice and presented in Table 1. ^{99m}Tc-RAD-Lys-(Arg^{11})CCMSH exhibited rapid and high tumor uptake in melanoma-bearing mice. The tumor uptake was 16.65 ± 1.91, 19.91 ± 4.02 and 18.01 ± 3.51% ID/g at 0.5, 2 and 4 h post-injection. In peptide blocking study, the tumor uptake of ^{99m}Tc-RAD-Lys-(Arg^{11})CCMSH with 10 μg (6.1 nmol) of non-radiolabeled NDP-MSH co-injection was only 7.8% of the tumor uptake without NDP-MSH co-injection at 2 h post-injection ($p<0.01$), demonstrating that the tumor uptake was specific and MC1 receptor-mediated. Whole-body clearance of ^{99m}Tc-RGD-Lys-(Arg^{11})CCMSH was rapid, with approximately 63% of the injected radioactivity cleared through the urinary system by 2 h post-injection (Table 1). Normal organ uptake of ^{99m}Tc-RGD-Lys-(Arg^{11})CCMSH was generally lower than 2.2% ID/g except for kidneys after 2 h post-injection. High tumor/blood and tumor/muscle uptake ratios were demonstrated as early as 0.5 h post-injection (Table 1). The renal uptake of ^{99m}Tc-RAD-Lys-(Arg^{11})CCMSH reached its peak value of 127.41 ± 17.32% ID/g at 0.5 h post-injection, and decreased to 33.19 ± 3.39% ID/g at 24 h post-injection.

In our previous report,[24] ^{99m}Tc-RGD-Lys-(Arg^{11})CCMSH displayed B16/F1 melanoma uptake of 11.06 ± 1.41, 14.83 ± 2.94 and 12.57 ± 2.53% ID/g at 0.5, 2 and 4 h post-injection, respectively. In this study, the switch from RGD to RAD significantly ($p<0.05$) improved the tumor uptake of ^{99m}Tc-RAD-Lys-(Arg^{11})CCMSH at 0.5, 2 and 4 h post-injection. The tumor uptake of ^{99m}Tc-RAD-Lys-(Arg^{11})CCMSH was 1.51, 1.34 and 1.43 times the tumor uptake of ^{99m}Tc-RGD-Lys-(Arg^{11})CCMSH at 0.5, 2 and 4 h post-injection (Fig. 4A), respectively. The improved melanoma uptake of ^{99m}Tc-RAD-Lys-(Arg^{11})CCMSH was likely due to its stronger MC1 receptor binding affinity compared to ^{99m}Tc-RGD-Lys-(Arg^{11})CCMSH (0.26 vs. 2.1 nM). Meanwhile, the replacement of the RGD motif with RAD significantly ($p<0.05$) decreased the liver uptake of ^{99m}Tc-RAD-Lys-(Arg^{11})CCMSH at 0.5, 4 and 24 h post-injection. The liver uptake of ^{99m}Tc-RAD-Lys-(Arg^{11})CCMSH was 66.2, 61.9 and 72.3% of the liver uptake of ^{99m}Tc-RGD-Lys-(Arg^{11})CCMSH at 0.5, 2 and 24 h post-injection (Fig. 4B), respectively.

Melanoma imaging property of ^{99m}Tc-RAD-Lys-(Arg^{11})CCMSH was examined in a B16/F1 melanoma-bearing C57 mouse in this study. The whole-body SPECT/CT image is presented in Figure 5. Flank melanoma tumors were visualized clearly by ^{99m}Tc-RAD-Lys-(Arg^{11})CCMSH at 2 h post-injection. ^{99m}Tc-RAD-Lys-(Arg^{11})CCMSH exhibited high tumor to normal organ uptake ratios except for kidney, which was consistent with the biodistribution results (Table 1). The urine collected from the imaging mouse was analyzed for the metabolites by HPLC. The urinary HPLC profile of ^{99m}Tc-RAD-Lys-(Arg^{11})CCMSH is shown in Figure 6. Approximately 82% of ^{99m}Tc-RAD-Lys-(Arg^{11})CCMSH remained intact, whereas 18% of ^{99m}Tc-RAD-Lys-(Arg^{11})CCMSH was transformed to a more lipophilic metabolite at 2 h post-injection.

As shown in Figure 4C, ^{99m}Tc-RAD-Lys-(Arg^{11})CCMSH exhibited significantly higher renal uptake than that of ^{99m}Tc-RGD-Lys-(Arg^{11})CCMSH at 0.5, 2 and 4 h post-injection. The renal uptake of ^{99m}Tc-RAD-Lys-(Arg^{11})CCMSH was 1.84. 1.39 and 1.42 times the renal uptake of ^{99m}Tc-RGD-Lys-(Arg^{11})CCMSH at 0.5, 2 and 4 h post-injection, respectively. Co-injection of peptide blockade did not reduce the renal uptake, indicating that the renal uptake of ^{99m}Tc-RAD-Lys-(Arg^{11})CCMSH was not MC1 receptor-mediated. *L*-lysine co-injection significantly decreased the renal uptake of ^{99m}Tc-RAD-Lys-(Arg^{11})CCMSH by 46%, demonstrating that *L*-lysine co-injection could be used to reduce the renal uptake of ^{99m}Tc-RAD-Lys-(Arg^{11})CCMSH. Importantly, the success of *L*-lysine co-injection suggested that the positive charge played a key role in the renal uptake of ^{99m}Tc-RAD-Lys-(Arg^{11})CCMSH. It was worthwhile to note that the epsilon amino group

of Lys linking the RAD motif and CCMSH contributed a positive charge to the overall charge of ^{99m}Tc-RAD-Lys-(Arg^{11})CCMSH. Reduction of the overall positive charge of radiolabeled α-MSH peptide via structural modification has been successfully utilized to decrease the renal uptake by 50%.[11] Accordingly, it would be likely to decrease the renal uptake of ^{99m}Tc-RAD-Lys-(Arg^{11})CCMSH by substituting the Lys linker with neutral amino acid or polyethylene glycol (PEG) linker in our future studies.

In conclusion, the substitution of Gly with Ala significantly enhanced the melanoma uptake of ^{99m}Tc-RAD-Lys-(Arg^{11})CCMSH compared to ^{99m}Tc-RGD-Lys-(Arg^{11})CCMSH in B16/F1 melanoma-bearing C57 mice. B16/F1 melanoma lesions were clearly visualized by SPECT/CT imaging using ^{99m}Tc-RAD-Lys-(Arg^{11})CCMSH as an imaging probe, highlighting its potential use as an imaging probe for melanoma detection.

The experimental details are presented in References and notes. [25-28]

Acknowledgments

We appreciate Dr. Fabio Gallazzi for his technical assistance. This work was supported in part by the NIH grant NM-INBRE P20RR016480, the University of New Mexico STC Gap Fund and the University of New Mexico RAC Award. The image in this article was generated by the Keck-UNM Small Animal Imaging Resource established with funding from the W.M. Keck Foundation and the University of New Mexico Cancer Research and Treatment Center (NIH P30 CA118100).

References and notes

1. Jemal A, Siegel R, Xu J, Ward E. CA Cancer J. Clin. 2010; 60:277. [PubMed: 20610543]
2. Giblin MF, Wang N, Hoffman TJ, Jurisson SS, Quinn TP. Proc. Natl. Acad. Sci. U.S.A. 1998; 95:12814. [PubMed: 9788997]
3. Froidevaux S, Calame-Christe M, Tanner H, Sumanovski L, Eberle AN. J. Nucl. Med. 2002; 43:1699. [PubMed: 12468522]
4. Miao Y, Whitener D, Feng W, Owen NK, Chen J, Quinn TP. Bioconjug. Chem. 2003; 14:1177. [PubMed: 14624632]
5. Froidevaux S, Calame-Christe M, Schuhmacher J, Tanner H, Saffrich R, Henze M, Eberle AN. J. Nucl. Med. 2004; 45:116. [PubMed: 14734683]
6. McQuade P, Miao Y, Yoo J, Quinn TP, Welch MJ, Lewis JS. J. Med. Chem. 2005; 48:2985. [PubMed: 15828837]
7. Wei L, Butcher C, Miao Y, Gallazzi F, Quinn TP, Welch MJ, Lewis JS. J. Nucl. Med. 2007; 48:64. [PubMed: 17204700]
8. Cheng Z, Xiong Z, Subbarayan M, Chen X, Gambhir SS. Bioconjug. Chem. 2007; 18:765. [PubMed: 17348700]
9. Miao Y, Benwell K, Quinn TP. J. Nucl. Med. 2007; 48:73. [PubMed: 17204701]
10. Miao Y, Figueroa SD, Fisher DR, Moore HA, Testa RF, Hoffman TJ, Quinn TP. J. Nucl. Med. 2008; 49:823. [PubMed: 18413404]
11. Miao Y, Gallazzi F, Guo H, Quinn TP. Bioconjug. Chem. 2008; 19:539. [PubMed: 18197608]
12. Guo H, Shenoy N, Gershman BM, Yang J, Sklar LA, Miao Y. Nucl. Med. Biol. 2009; 36:267. [PubMed: 19324272]
13. Guo H, Yang J, Gallazzi F, Miao Y. J. Nucl. Med. 2010; 51:418. [PubMed: 20150256]
14. Guo H, Yang J, Gallazzi F, Miao Y. J. Nucl. Med. 2011; 52:608. [PubMed: 21421725]
15. Haubner R, Wester HJ, Reuning U, Senekowitsch-Schmidtke R, Diefenbach B, Kessler H, Stöcklin G, Schwaiger M. J. Nucl. Med. 1999; 40:1061. [PubMed: 10452325]
16. Poethko T, Schottelius M, Thumshirn G, Hersel U, Herz M, Henriksen G, Kessler H, Schwaiger M, Wester HJ. J. Nucl. Med. 2004; 45:892. [PubMed: 15136641]
17. Li C, Wang W, Wu Q, Ke S, Houston J, Sevick-Muraca E, Dong L, Chow D, Charnsangavej C, Gelovani JG. Nucl. Med. Biol. 2006; 33:349. [PubMed: 16631083]

18. Decristoforo C, Faintuch-Linkowski B, Rey A, von Guggenberg E, Rupprich M, Hernandez-Gonzales I, Rodrigo T, Haubner R. Nucl. Med. Biol. 2006; 33:945. [PubMed: 17127166]
19. Alves S, Correia JD, Gano L, Rold TL, Prasanphanich A, Haubner R, Rupprich M, Alverto R, Decristoforo C, Santos I, Smith C. J. Bioconjug. Chem. 2007; 18:530.
20. Decristoforo C, Hernandez Gonzalez I, Carlsen J, Rupprich M, Huisman M, Virgolini I, Wester HJ, Haubner R. Eur. J. Nucl. Med. Mol. Imaging. 2008; 35:1507. [PubMed: 18369617]
21. Hultsch C, Schottelius M, Auernheimer J, Alke A, Wester HJ. Eur. J. Nucl. Med. Mol. Imaging. 2009; 36:1469. [PubMed: 19350236]
22. Wei L, Ye Y, Wadas TJ, Lewis JS, Welch MJ, Achilefu S, Anderson CJ. Nucl. Med. Biol. 2009; 36:277. [PubMed: 19324273]
23. Yang J, Guo H, Miao Y. Nucl. Med. Biol. 2010; 37:873–883. [PubMed: 21055617]
24. Yang J, Guo H, Gallazzi F, Berwick M, Padilla RS, Miao Y. Bioconjug. Chem. 2009; 20:1634. [PubMed: 19552406]
25. MC1 receptor binding affinity: Amino acid and resin were purchased from Advanced ChemTech Inc. (Louisville, KY) and Novabiochem (San Diego, CA). ^{125}I-Tyr^{2}-[Nle^{4}, $_{D}$Phe^{7}]-α-MSH {^{125}I-(Tyr^{2})-NDP-MSH} was obtained from PerkinElmer, Inc. (Shelton, CT) for MC1 receptor binding assay. B16/F1 murine melanoma cells were obtained from American Type Culture Collection (Manassas, VA). The RAD-Lys-(Arg^{11})CCMSH was synthesized, purified by reverse phase-high performance liquid chromatography (RP-HPLC) and characterized by LC-mass spectroscopy according to our published procedure.[23] The IC_{50} value of RAD-Lys-(Arg^{11})CCMSH for the MC1 receptor was determined in B16/F1 melanoma cells according to our published procedure[23] with modifications. Briefly, the B16/F1 cells (0.2×10^{6} cells/well, n=3) were incubated at 25 °C for 2 h with approximately 30,000 counts per minute (cpm) of ^{125}I-(Tyr^{2})-NDP-MSH in the presence of 10^{-13} to 10^{-6} M of RAD-Lys-(Arg^{11})CCMSH in 0.3 mL of binding medium. The medium was aspirated after the incubation. The cells were rinsed twice with 0.5 mL of ice-cold pH 7.4, 0.2% BSA/0.01 M phosphate buffered saline (PBS) and lysed in 0.5 mL of 1 N NaOH for 5 min. The cells were collected and counted in a Wallac 1480 automated gamma counter (PerkinElmer, NJ). The IC_{50} value of RAD-Lys-(Arg^{11})CCMSH was calculated using the Prism software (GraphPad Software, La Jolla, CA).
26. Cellular internalization and efflux of ^{99m}Tc-RAD-Lys-(Arg^{11})CCMSH: $^{99m}TcO_4^-$ was purchased from Cardinal Health (Albuquerque, NM) for peptide radiolabeling. All other chemicals used in this study were purchased from Thermo Fisher Scientific (Waltham, MA) and used without further purification. RAD-Lys-(Arg^{11})CCMSH was radiolabeled with ^{99m}Tc using the method described previously.[23] The radiolabeled peptide was purified to single species by Waters RP-HPLC (Milford, MA) on a Grace Vydac C-18 reverse phase analytic column (Deerfield, IL) using a 20 min gradient of 16-26% acetonitrile in 20 mM HCl aqueous solution at a flow rate of 1 mL/min. Cellular internalization and efflux of ^{99m}Tc -RAD-Lys-(Arg^{11})CCMSH were evaluated in B16/F1 melanoma cells according to our published procedure.[24]
27. **Biodistribution studies**: All the animal studies were conducted in compliance with Institutional Animal Care and Use Committee approval. The biodistribution of ^{99m}Tc-RAD-Lys-(Arg^{11})CCMSH was determined in B16/F1 melanoma-bearing C57 mice (Harlan, Indianapolis, IN). C57 mice were subcutaneously inoculated on the right flank with 1×10^{6} B16/F1 cells. Tumor weights reached approximately 0.2 g at 10 days post cell inoculation. Each melanoma-bearing mouse was injected with 0.037 MBq of ^{99m}Tc-RAD-Lys-(Arg^{11})CCMSH via the tail vein. Groups of 5 mice were sacrificed at 0.5, 2, 4 and 24 h post-injection, and tumors and organs of interest were harvested, weighed and counted. Blood values were taken as 6.5% of the whole-body weight. The specificity of tumor uptake was determined at 2 h post-injection by co-injecting ^{99m}Tc-RAD-Lys-(Arg^{11})CCMSH with 10 μg (6.1 nmol) of unlabeled NDP-MSH. *L*-lysine co-injection is effective in decreasing the renal uptake of radiolabeled α-MSH peptides. To determine the effect of *L*-lysine co-injection on the renal uptake of ^{99m}Tc-RAD-Lys-(Arg^{11})CCMSH, a group of 5 mice were injected with a mixture of 0.037 MBq of ^{99m}Tc-RAD-Lys-(Arg^{11})CCMSH and 12 mg of *L*-lysine. The mice were sacrificed at 2 h post-injection, and tumors and organs of interest were harvested, weighed and counted in a gamma counter. Statistical analysis was performed using the Student's t-test for unpaired data to determine the significance of differences in tumor and kidney uptake between the groups in the biodistribution studies with/

without peptide blockade or with/without *L*-lysine co-injection. Differences at the 95% confidence level ($p<0.05$) were considered significant.

28. Melanoma imaging and urinary metabolites of ^{99m}Tc-RAD-Lys-(Arg^{11})CCMSH: Approximately 6.7 MBq of ^{99m}Tc-RAD-Lys-(Arg^{11})CCMSH was injected in a B16/F1 melanoma-bearing C57 mouse for imaging and urine analysis. The mouse was euthanized at 2 h post-injection for small animal SPECT/CT (Nano-SPECT/CT®, Bioscan) imaging, as well as to collect urine for analyzing the metabolites. The 9-min CT imaging was immediately followed by the whole-body SPECT scan. The SPECT scans of 24 projections were acquired. Reconstructed SPECT and CT data were visualized and co-registered using InVivoScope (Bioscan, Washington DC). The collected urine sample was centrifuged at 16,000 *g* for 5 min before the HPLC analysis. Thereafter, aliquots of the urine were injected into the HPLC. A 20-minute gradient of 16-26% acetonitrile/20 mM HCl with a flow rate of 1 mL/min was used for urine analysis.

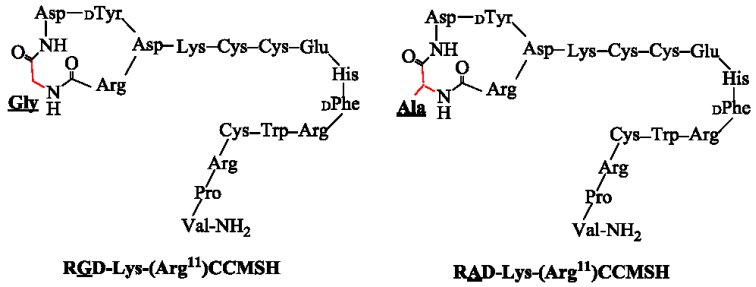

Figure 1.
Schematic structures of RAD-Lys-(Arg^{11})CCMSH and RGD-Lys-(Arg^{11})CCMSH.

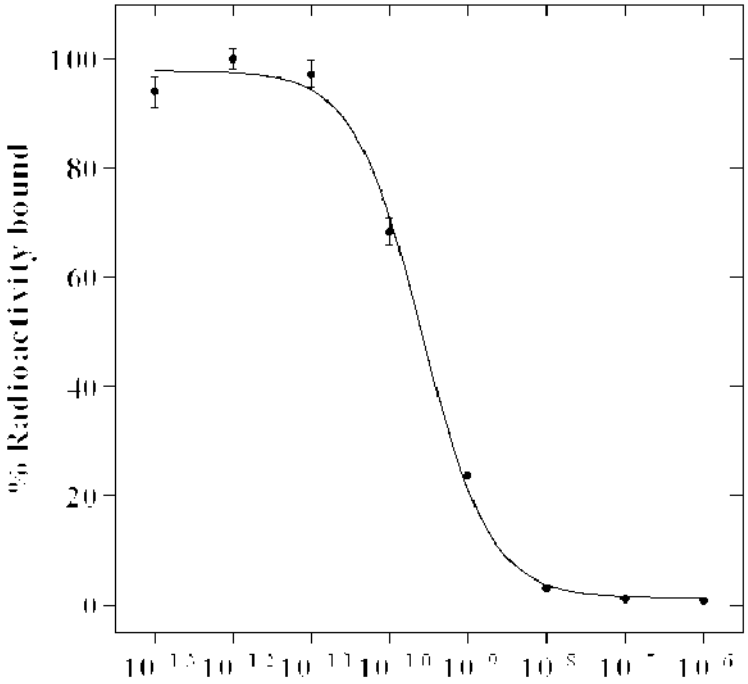

Figure 2.
The competitive binding curve of RAD-Lys-(Arg^{11})CCMSH in B16/F1 melanoma cells. The IC_{50} value of RAD-Lys-(Arg^{11})CCMSH was 0.26 nM.

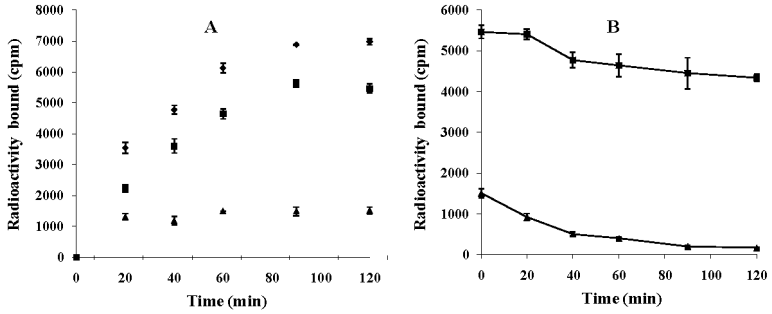

Figure 3.

Cellular internalization (A) and efflux (B) of ^{99m}Tc-RAD-Lys-(Arg^{11})CCMSH in B16/F1 melanoma cells. Total bound radioactivity (◆), internalized radioactivity (■) and cell membrane radioactivity (▲) were presented as counts per minute (cpm).

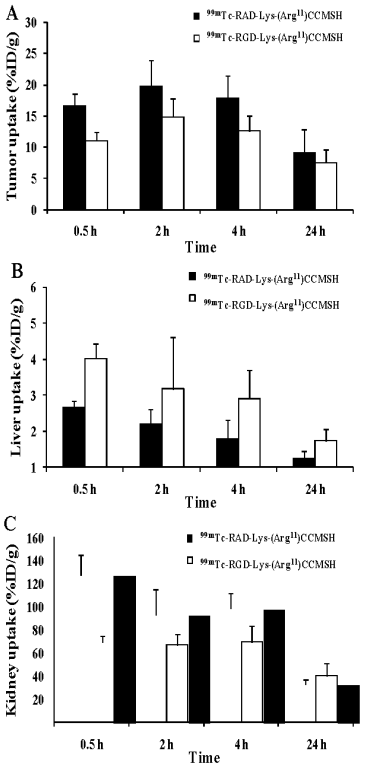

Figure 4.

Comparison in tumor, liver and kidney uptake between ^{99m}Tc-RAD-Lys-(Arg^{11})CCMSH and ^{99m}Tc-RGD-Lys-(Arg^{11})CCMSH. The data of ^{99m}Tc-RGD-Lys-(Arg^{11})CCMSH was cited from our previous report.[24]

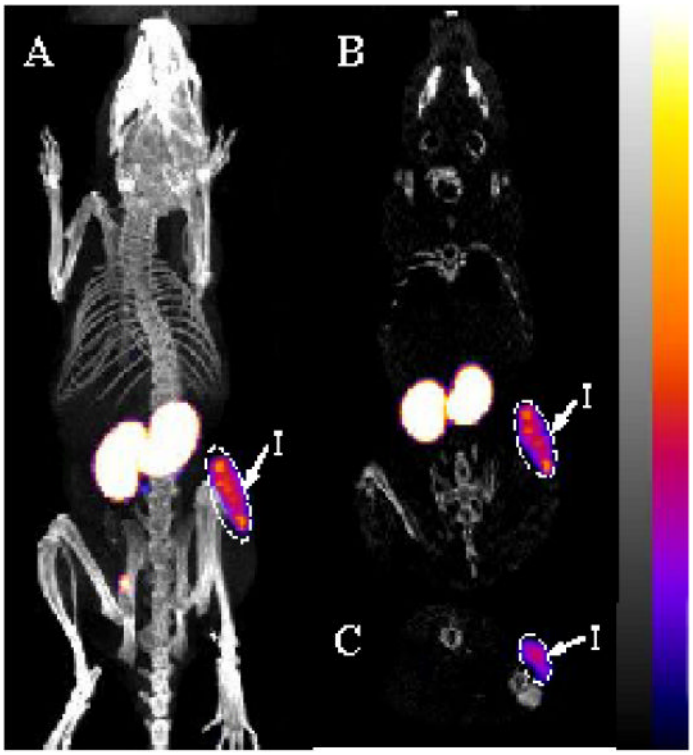

Figure 5.
Whole-body (A), coronal (B) and transversal (C) SPECT/CT images of ^{99m}Tc-RAD-Lys-(Arg^{11})CCMSH in a B16/F1 melanoma-bearing C57 mouse at 2 h post-injection. Flank melanoma lesions (T) were highlighted with arrows on the images.

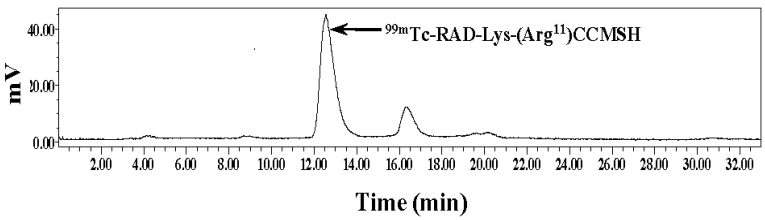

Figure 6.

Radioactive HPLC profile of urine sample of a B16/F1 melanoma-bearing C57 mouse at 2 h post-injection of ^{99m}Tc-RAD-Lys-(Arg^{11})CCMSH. Arrow indicates the retention time (12.6 min) of the original compound of ^{99m}Tc-RAD-Lys-(Arg^{11})CCMSH prior to the tail vein injection.

Bioorg Med Chem Lett. Author manuscript; available in PMC 2013 February 15.

Table 1

Biodistribution of ^{99m}Tc-RAD-Lys-(Arg^{11})CCMSH in B16/F1 melanoma-bearing C57 mice. The data was presented as percent injected dose/gram or as percent injected dose (mean±SD, n=5)

Tissue	0.5 h	2 h	4 h	24 h	2 h NDP blockade	2 h *L*-lysine co-injection
			Percent injected dose/gram (%ID/g)			
Tumor	16.65 ± 1.91	19.91 ± 4.02	18.01 ± 3.51	9.24 ± 3.63	1.55 ± 0.71 *	18.62 ± 1.73
Brain	0.14 ± 0.03	0.04 ± 0.01	0.02 ± 0.00	0.02 ± 0.01	0.02 ± 0.02	0.04 ± 0.01
Blood	3.46 ± 0.50	0.49 ± 0.31	0.20 ± 0.09	0.05 ± 0.02	0.67 ± 0.17	0.44 ± 0.11
Heart	2.12 ± 0.46	0.32 ± 0.13	0.20 ± 0.08	0.13 ± 0.04	0.32 ± 0.15	0.30 ± 0.10
Lung	3.91 ± 1.37	0.87 ± 0.21	0.46 ± 0.11	0.29 ± 0.07	1.49 ± 0.37	0.78 ± 0.17
Liver	2.66 ± 0.17	2.22 ± 0.39	1.80 ± 0.51	1.25 ± 0.20	4.17 ± 1.36	1.46 ± 0.08
Skin	4.71 ± 0.49	0.71 ± 0.25	0.34 ± 0.05	0.26 ± 0.15	0.85 ± 0.58	0.58 ± 0.10
Spleen	1.54 ± 0.41	0.48 ± 0.21	0.37 ± 0.26	0.39 ± 0.24	0.58 ± 0.72	0.50 ± 0.09
Stomach	2.50 ± 0.16	1.61 ± 0.35	1.09 ± 0.37	0.51 ± 0.22	2.37 ± 0.35	1.92 ± 0.24
Kidneys	127.41 ± 17.32	92.97 ± 21.72	98.56 ± 13.49	33.19 ± 3.39	74.13 ± 16.15	50.10 ± 18.56 *
Muscle	0.72 ± 0.18	0.14 ± 0.08	0.18 ± 0.04	0.08 ± 0.04	0.32 ± 0.04	0.28 ± 0.30
Pancreas	0.95 ± 0.38	0.19 ± 0.05	0.12 ± 0.05	0.02 ± 0.07	0.23 ± 0.09	0.14 ± 0.04
Bone	1.75 ± 0.29	0.37 ± 0.21	0.17 ± 0.08	0.11 ± 0.08	0.40 ± 0.27	0.52 ± 0.31
			Percent injected dose (%ID)			
Intestines	2.15 ± 0.25	1.50 ± 0.86	1.55 ± 0.42	0.85 ± 0.42	3.89 ± 1.31	1.31 ± 0.31
Bladder	30.95 ± 5.12	65.84 ± 7.08	65.69 ± 4.62	85.62 ± 1.21	69.54 ± 0.63	70.34 ± 3.28
			Uptake ratio of tumor/normal tissue			
Tumor/Blood	4.81	40.63	90.05	184.80	2.31	42.32
Tumor/Kidneys	0.13	0.21	0.18	0.28	0.02	0.37
Tumor/Lung	4.26	22.89	39.15	31.86	1.04	23.87
Tumor/Liver	6.26	8.97	10.01	7.39	0.37	12.75
Tumor/Muscle	23.13	142.21	100.06	115.50	4.84	66.50

* $p<0.05$, significance comparison in tumor and kidney between ^{99m}Tc-RAD-Lys-(Arg^{11})CCMSH with/without peptide blockade and with/without *L*-lysine co-injection at 2 h post-injection.